AIP Journal of Applied Physics

Tailoring thermal expansion in metal matrix composites blended by antiperovskite manganese nitrides exhibiting giant negative thermal expansion

K. Takenaka, T. Hamada, D. Kasugai, and N. Sugimoto

Citation: Journal of Applied Physics **112**, 083517 (2012); doi: 10.1063/1.4759121
View online: http://dx.doi.org/10.1063/1.4759121
View Table of Contents: http://scitation.aip.org/content/aip/journal/jap/112/8?ver=pdfcov
Published by the AIP Publishing

Tailoring thermal expansion in metal matrix composites blended by antiperovskite manganese nitrides exhibiting giant negative thermal expansion

K. Takenaka,[a] T. Hamada, D. Kasugai, and N. Sugimoto
Department of Crystalline Materials Science, Nagoya University, Nagoya 464-8603, Japan

(Received 17 July 2012; accepted 19 September 2012; published online 22 October 2012)

We controlled thermal expansion of metal matrix composites (MMCs) that had been blended using antiperovskite manganese nitrides with giant negative thermal expansion (NTE). The NTE of the manganese nitrides, which is isotopic, is greater than $-30\,\text{ppm}\,\text{K}^{-1}$ in α (coefficient of linear thermal expansion), which is several or ten times as large as that of conventional NTE materials. These advantages of nitrides are desirable for practical application as a thermal-expansion compensator, which can suppress thermal expansion of various materials including metals and even plastics. Powder metallurgy using pulsed electric current sintering enables us to reduce temperatures and times for fabrication of MMCs. Consequently, chemical reactions between matrix (Al, Ti, Cu) and filler can be controlled and even high-melting-point metals can be used as a matrix. Thermal expansion of these MMCs is tunable across widely various α values, even negative ones, with high reproducibility. These composites retain a certain amount of voids. Formation of rich and stable interfacial bonding, overcoming large mismatch in thermal expansion, remains as a problem that is expected to hinder better composite performance. © *2012 American Institute of Physics*. [http://dx.doi.org/10.1063/1.4759121]

I. INTRODUCTION

Significant recent advances in technology require industrial materials that are capable of withstanding severe conditions. Although thermal expansion is typically 10^{-5} to 10^{-6} in length, even such a minute change fatally degrades the performance of devices and instruments in high-precision industries such as Ultra-Large Scale Integration (ULSI) fabrication. Furthermore, for a device comprising plural materials, mismatch in thermal expansion between the constituents themselves causes severe damage such as exfoliation of interfaces or breakage of wires. Consequently, strong demand exists to adjust thermal expansion of a material to some particular value, typically zero, in many fields of engineering, including machining and processing, optics, and electronics. Furthermore, for "green" technologies such as fuel cells and thermoelectric converters, control of thermal expansion in joints is a key issue for high performance.

For control of thermal expansion, composites of various types containing a low thermal expansion filler have been designed.[1–3] However, because thermal expansion of a typical filler silica (SiO_2) is, although low, still positive (coefficient of linear thermal expansion α, CTE, being 0.5 ppm K^{-1}), thermal expansion of the matrix is not compensated. For a wider range of control in thermal expansion, *negative* thermal expansion (NTE) materials are necessary: materials that contract on heating.[4] To this end, silicates of a certain group, such as β-eucryptite ($LiAlSiO_4$), have been used.[5–7] The NTE of such silicates, however, is highly anisotropic and the magnitude of net NTE is small (several parts per million K^{-1} in α),[8] compared with positive thermal expansion of metals ($\alpha = 10 - 20\,\text{ppm}\,\text{K}^{-1}$) or plastics (at least $\alpha = 30 - 40\,\text{ppm}\,\text{K}^{-1}$ and sometimes greater than $100\,\text{ppm}\,\text{K}^{-1}$). Therefore their ability of thermal-expansion compensation remains limited. Large ($\alpha = -9$ ppm K^{-1}) and isotropic NTE of ZrW_2O_8 (Ref. 9) are anticipated for more effective control of thermal expansion of materials,[10–17] but the unfavorable structural deformation degrades the performance of thermal-expansion compensation.

Research on NTE materials has shown remarkable progress during the last decade. Particularly after the discovery of giant NTE in antiperovskite manganese nitrides Mn_3AN (A: transition metal or semiconducting element),[18] materials exhibiting giant NTE were discovered successively.[19–22] The NTE of Mn_3AN is greater than $-30\,\text{ppm}\,\text{K}^{-1}$ in α, which has at last become capable of cancelling the thermal expansion of various materials, even plastics. Such giant NTE is opening a new phase of composite science and technology.[23,24]

This report describes adjustable thermal expansion in a metal matrix composite (MMC) comprising giant NTE manganese nitride as a thermal expansion compensating filler. Pulsed electric current sintering reduces fabrication temperatures of MMC to far below the melting point of metal matrices, thereby enabling the use of metals with a high melting point as a matrix. The giant NTE of Mn_3AN controlled the overall thermal expansion of the MMCs across widely various α values, including even negative ones. We discuss conditions of forming the composites, their thermal-expansion properties, chemistry and physics of the interfaces, and future prospects.

II. PROCEDURES

Thermal-expansion compensators, antiperovskite manganese nitrides, were prepared using solid-state reactions.[25]

[a]Electronic address: takenaka@nuap.nagoya-u.ac.jp.

TABLE I. Physical properties of metal matrices and thermal-expansion compensators.

Material	Melting point T_m(°C)	Density d(g/cm^3)	CTE α(ppm/K)	Young's modulus E (GPa)	Vickers hardness H_V (kgf/mm^2)
Al	660	2.7	23.1	70	29
Ti	1675	4.5	8.4	115	152
Cu	1083	8.9	16.4	110	56
$Mn_{3.1}Zn_{0.5}Sn_{0.4}N$	–	7.0	7.5 (100–335 K) −36.4 (335–375 K) 23.8 (375–500 K)	200	400
$Mn_{3.27}Zn_{0.45}Sn_{0.28}N$	–	7.0	6.3 (100–325 K) −30.3 (265–325 K) 23.8 (325–500 K)	200	400

First we obtained stoichiometric Mn_3AN (A: Cu, Zn, Sn). Powders of Mn_2N and pure element A (purity: 99.9% or higher) were mixed in a bag filled with nitrogen gas and then sealed in a quartz tube under vacuum ($<10^{-3}$ Torr). The sealed quartz tube was heated at temperature $T = 500-760$ °C for 40–70 h. The nitrogen pressure in the quartz tube was kept higher than 1 atm because of decomposition of Mn_2N. Mn_4N was obtained by heating pure Mn powder (99.9% purity) at 450 °C for 80 h in a gas flow of purified nitrogen. The stoichiometric antiperovskites were mixed in an appropriate molar ratio, sealed in a quartz tube under vacuum, and heated at 800 °C for 60 h. [For example, we obtained $Mn_{3.1}Zn_{0.5}Sn_{0.4}N$ using a mixture of Mn_3ZnN, Mn_3SnN, and Mn_4N in a molar ratio of 5:4:1]. The obtained nitride powder was sintered for measurement of linear thermal expansion $\Delta L(T)/L$ using a spark plasma sintering (SPS) furnace (Syntex Lab; SPS Syntex Inc.). The sintering was conducted using a graphite die at 600 °C for 10 min under vacuum ($<10^{-3}$ Torr). The sintered specimen was cut into a rectangular shape (typically $5 \times 5 \times 12$ mm^3) and $\Delta L(T)/L$ was measured at 100–500 K using a laser-interference dilatometer (LIX-2; Ulvac). The accuracy of the length change measurement using this dilatometer was 20 nm, which is equivalent to less than 10^{-7} K^{-1} in α.[26,27] The crystal structure was investigated using x-ray powder diffraction (XRD, RINT2000; Rigaku).

The obtained nitride thermal-expansion compensator was pulverized down to 30–50 μm diameter. We mixed powders of the thermal-expansion compensator and metal matrix in an appropriate volume ratio, packed them in a graphite die, and installed it in the SPS furnace. Then sintering was conducted under vacuum ($<10^{-3}$ Torr). The sintered MMC sample was cut into a rectangular shape (typically $5 \times 5 \times 12$ mm^3) and $\Delta L(T)/L$ was measured at 100–500 K using the laser-interference dilatometer. To verify the chemical reaction between the metal matrix and the thermal-expansion compensator, we powdered the MMC sample using a diamond file and ascertained the XRD pattern. The physical properties of the metal matrices and the thermal-expansion compensators are presented in Table I and fabrication parameters for composites are presented in Table II.

The measured thermal expansion of MMC was analyzed using models in which particles of an isotropic thermal-expansion compensator are dispersed uniformly in an isotropic matrix.[28] Here, we, respectively, define subscripts c, m, and t as the composite, matrix, and thermal-expansion compensator. A bound of α_c is given, assuming that thermally induced stress is uniform everywhere in a composite, which is equivalent to the assumption that the matrix and thermal-expansion compensator exhibit their own thermal expansion independently. Consequently, thermal expansion of a composite is given by the volume-weighted sum of the contributions from matrix and the dispersed phase.

$$\alpha_c = v_m\alpha_m + v_t\alpha_t. \quad (1)$$

Here, v_m and v_t, respectively, denote the volume fractions of the matrix and thermal-expansion compensator, and $v_m + v_t = 1$, which is called the rule of mixture (ROM). Another bound is given by the approximation that thermally induced strain is uniform throughout a composite because of the interfacial elastic interactions between the matrix and thermal-expansion compensator, as first proposed by Turner[29]:

$$\alpha_c = \frac{v_m E_m \alpha_m + v_t E_t \alpha_t}{v_m E_m + v_t E_t}. \quad (2)$$

Here, E_m and E_t, respectively, denote Young's moduli of the matrix and thermal-expansion compensator. In Eq. (2), the constituent with the larger elastic modulus contributes more to α_c beyond the volume fraction. For the manganese nitrides, the Young's modulus is greater than 200 GPa[30] and the relations $\alpha_m > \alpha_t$ and $E_m < E_t$ are always fulfilled (Table I). Therefore, Eq. (1), ROM, gives the upper bound and Eq. (2), Turner's model, gives the lower bound for α_c in this case. In the following, thermal expansion of the composites is evaluated based on $\Delta L(T)/L$ (integral of α) instead of α because α of these composites drastically changes around the operating temperature of NTE in the manganese-nitride filler. Therefore, the overall thermal expansion is a more appropriate indicator of the composite performance.

TABLE II. Fabrication parameters for composites.

Matrix	Temperature T_s(°C)	Time t_s(min)	Pressure p_s(MPa)	Particle size r(μm)
Al	350	7	40	3
Ti	650	7	30	45
Cu	550	7	30	1

III. RESULTS

A. Thermal-expansion compensator

Figure 1 displays linear thermal expansion $\Delta L(T)/L$ for the thermal-expansion compensator, $Mn_{3+x}Zn_ySn_{1-x-y}N$ (Mn-Zn-Sn-N). The giant NTE of the manganese nitrides was achieved by doping Ge or Sn into A site as "relaxant" of the sharp volume change caused by the first-order magnetic transition.[18,25,31–33] Now the role of elements at the A site has been clarified. We can tune the thermal expansion by combination of the element that expands the lattice at the onset of magnetic ordering (Cu, Zn, Ga, etc.) and the element that relaxes the sharp volume change (Ge, Sn). We used $Mn_{3+x}Zn_ySn_{1-x-y}N$ as the most practical thermal-expansion compensator in terms of functionality as well as cost.[34] The magnitude of the volume expansion of Mn-Zn-Sn-N is more than twice as large as that of another practical NTE compound $Mn_{3+x}Cu_ySn_{1-x-y}N$ (Mn-Cu-Sn-N). $Mn_{3.1}Zn_{0.5}Sn_{0.4}N$ shows NTE of $\alpha = -36.4$ ppm K^{-1} at $T = 335$–375 K (operating-temperature window $\Delta T = 40$ K) and $Mn_{3.27}Zn_{0.45}Sn_{0.28}N$ shows NTE of $\alpha = -30.3$ ppm K^{-1} at $T = 265$–325 K ($\Delta T = 60$ K), while a typical NTE compound $Mn_3Cu_{0.5}Sn_{0.5}N$ shows NTE of $\alpha = -27.8$ ppm K^{-1} at $T = 305$–335 K ($\Delta T = 30$ K). The Zn-based compounds exhibit better performance than the Cu counterpart in terms of the magnitude of NTE and width of ΔT.

B. Mn-Zn-Sn-N/Al composite

Before fabrication of MMCs, we determined the sintering temperature T_s of pure metal matrices. Figure 2(a) displays the displacement during the densification of Al powder using SPS at 40 MPa. The negative displacement corresponds to the decrease in volume of the powder packed in the graphite die. The magnitude of the displacement increased as T rose, but it saturated above 300 °C. Therefore, the sintering of Al finished at 300 °C, which is much lower than the melting point T_m of Al, 660 °C (Table II). We measured the displacement during densification of the 30 vol. %-$Mn_{3.1}Zn_{0.5}Sn_{0.4}N$/Al mixed powder [Fig. 2(b)]. The magnitude of the displacement increased gradually from 250 °C. Even after 300 °C, the magnitude of the displacement continued to increase, which is interpreted as a sign of the filler/matrix interfacial chemical reaction. At 520 °C, the magnitude of the displacement increased abruptly. We also verified that the pure manganese nitrides can be sintered at $T = 480-650$ °C. Therefore, the abrupt increase can be explained partly as the onset of sintering between the manganese-nitride particles themselves. However, as described later, the abrupt change at 520 °C is ascribed more reasonably to the onset of progressive chemical reaction between the matrix and the compensator.

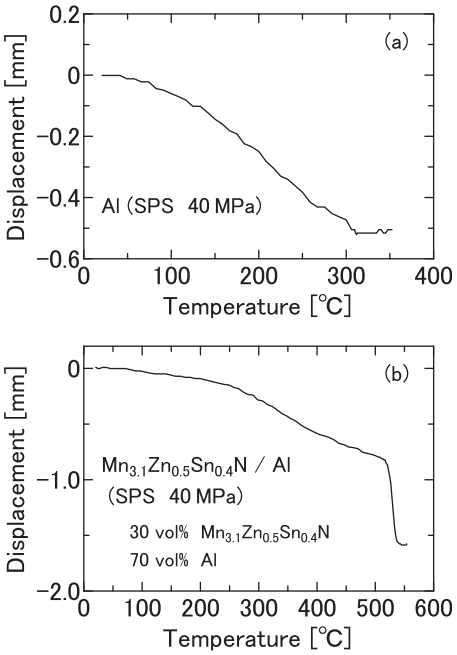

FIG. 2. Displacement during the densification of pure aluminum powder (a) and 30 vol. %-$Mn_{3.1}Zn_{0.5}Sn_{0.4}N$/Al composite using spark plasma sintering (sintering pressure $p_s = 40$ MPa).

Based on these preliminary experiments, we attempted to fabricate the Al matrix composites at $T_s = 350-550$ °C during a fixed sintering time $t_s = 7$ min. Figure 3 displays the T_s dependence of $\Delta L(T)/L$ for the 30 vol. %-$Mn_{3.1}Zn_{0.5}Sn_{0.4}N$/Al composites. The data for $T_s = 350$ °C and 450 °C are identical. The thermal expansion was suppressed by giant NTE of $Mn_{3.1}Zn_{0.5}Sn_{0.4}N$, resulting in an even negative slope ($\alpha = -6.1$ ppm K^{-1}) at $T = 345$–370 K ($\Delta T = 25$ K).

By contrast, the data for $T_s = 550$ °C exhibit positive thermal expansion over a whole T range. Both the matrix and the thermal-expansion compensator show almost identical thermal expansion at temperatures higher than the operating

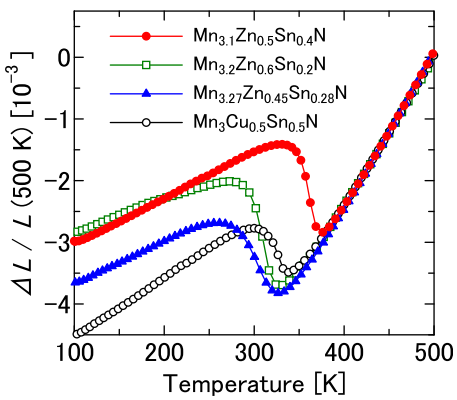

FIG. 1. Liner thermal expansion of typical antiperovskite manganese nitrides showing negative thermal expansion.

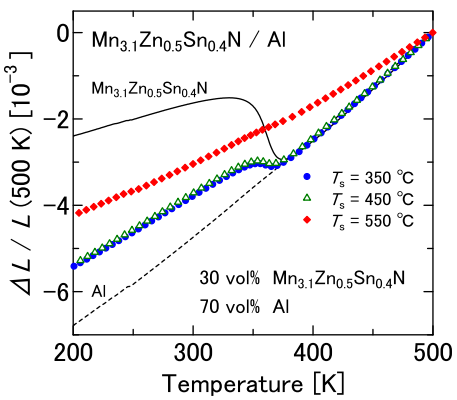

FIG. 3. Linear thermal expansion of 30 vol. %-$Mn_{3.1}Zn_{0.5}Sn_{0.4}N$/Al composite for different fabrication temperatures T_s.

temperature window ($T > 375$ K). Therefore, the composites are expected to exhibit the same thermal expansion as that of the matrix and the compensator at this T range. It is true for $T_s = 350\,^{\circ}$C and $450\,^{\circ}$C. However, it does not hold for $T_s = 550\,^{\circ}$C, suggesting a chemical reaction between the matrix and the compensator that occurs during sintering.

The chemical reaction at $T_s = 550\,^{\circ}$C was confirmed using XRD (Fig. 4). For $T_s = 350\,^{\circ}$C and $450\,^{\circ}$C the XRD profile after sintering is a superimposition of the individual patterns of the matrix and the compensator, whereas the profile for $T_s = 550\,^{\circ}$C differs greatly from that, exhibiting rather diffusive, unknown-phase peaks without those of the matrix or the compensator. The microscope observation also supports the chemical reaction at $T_s = 550\,^{\circ}$C (Fig. 5). For $T_s = 350\,^{\circ}$C and $450\,^{\circ}$C, we distinguish between the matrix (matte gray), the compensator (glossy gray), and the voids (black). For $T_s = 550\,^{\circ}$C, the glossy parts disappeared and the whole body became matte, including different colored grains here and there, while the voids decreased. The results show that $550\,^{\circ}$C is too high for fabrication of the Mn-Zn-Sn-N/Al composite because of progressive chemical reaction between the matrix and the compensator.

Based on the results described above, we used $350\,^{\circ}$C as the fabrication temperature T_s for the Mn-Zn-Sn-N/Al composite. Then we examined effects of the sintering time t_s under the condition of the fixed sintering temperature $T_s = 350\,^{\circ}$C. Figure 6 displays the t_s dependence of $\Delta L(T)/L$ for the 30 vol. %-$Mn_{3.1}Zn_{0.5}Sn_{0.4}N$/Al composites. Although we altered t_s from 2 to 120 min, $\Delta L(T)/L$ is independent of t_s, which demonstrates not only insensitivity to the sintering time t_s, at least in the present t_s range, but also high reproducibility in thermal expansion of this composite. We also confirmed stability against thermal cycling. Results of $\Delta L(T)/L$ remained unchanged, although the measurements were taken three times (Fig. 7).

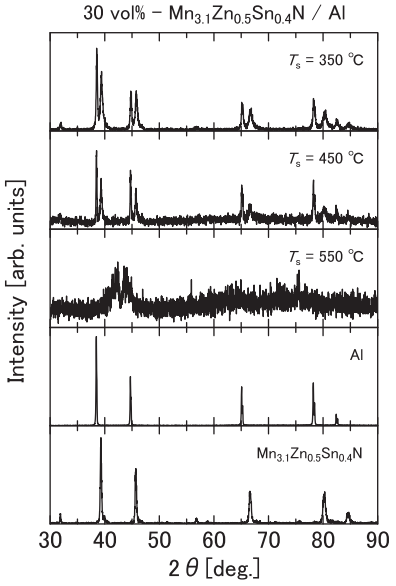

FIG. 4. X-ray diffraction profiles of 30 vol. %-$Mn_{3.1}Zn_{0.5}Sn_{0.4}N$/Al composite for different T_s. Profiles of pure Al and $Mn_{3.1}Zn_{0.5}Sn_{0.4}N$ are also shown for comparison.

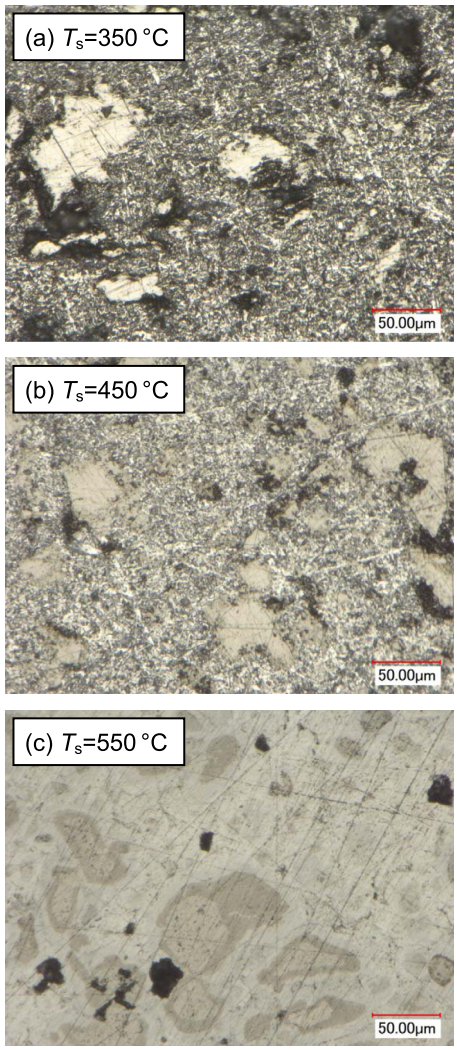

FIG. 5. Microscopic images of 30 vol. %-$Mn_{3.1}Zn_{0.5}Sn_{0.4}N$/Al composite for $T_s = 350\,^{\circ}$C (a), $450\,^{\circ}$C (b), and $550\,^{\circ}$C (c).

The performance of thermal-expansion compensator is examined based on two models: ROM and Turner's model. Figure 8 displays a plot of the $\Delta L(T)/L$ experimental values as well as the curves calculated assuming ROM and Turner's model. ROM gives the *minimum* $\Delta L(T)/L$ and Turner's model gives the *maximum* $\Delta L(T)/L$ for the present Al-matrix composites because the reference temperature of

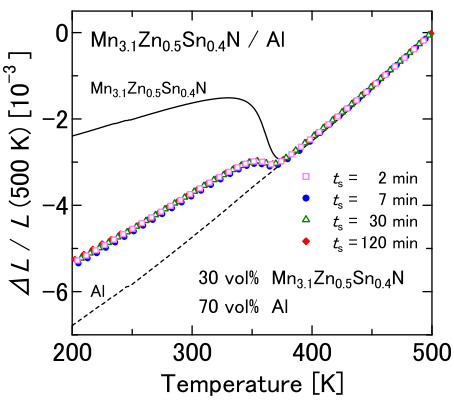

FIG. 6. Linear thermal expansion of 30 vol. %-$Mn_{3.1}Zn_{0.5}Sn_{0.4}N$/Al composite for different fabrication times t_s.

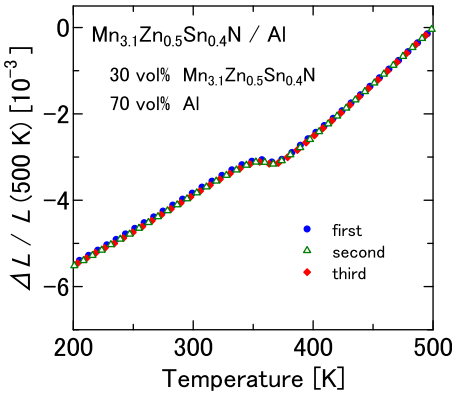

FIG. 7. Thermal cycling of linear thermal expansion for 30 vol. %-$Mn_{3.1}Zn_{0.5}Sn_{0.4}N$/Al composite.

$\Delta L(T)/L$, 500 K, is higher than the operating temperature of NTE, and α_m and α_t are identical above the operating temperature. The obtained $\Delta L(T)/L$ of the Mn-Zn-Sn-N/Al composite almost coincides with the ROM estimation. Therefore, additional suppression of thermal expansion beyond the volume fraction attributable to the high stiffness of the manganese nitride is not confirmed in this composite.

C. Mn-Zn-Sn-N/Ti composite

An important merit of SPS is that it forms composites at much lower temperatures than the melting point of a metal matrix. In this section, we present results of Ti matrix, the melting point of which is much higher than Al (Table I). Based on similar preliminary experiments, we fixed the fabrication parameters as $T_s = 650\,^{\circ}C$ and $t_s = 7$ min. We fabricated the Mn-Zn-Sn-N/Ti composites in widely various filler loading 10–90 vol. % [Fig. 9(a)]. We can achieve an arbitrary α value between 8.4 ppm K^{-1} (pure Ti) and -36.4 ppm K^{-1} (pure $Mn_{3.1}Zn_{0.5}Sn_{0.4}N$) for the Ti composite at $T = 340$–370 K ($\Delta T = 30$ K).

However, the thermal expansion of the composite is unreasonably higher than the upper bound of the simple models. Figure 9(b) displays a plot of the $\Delta L(T)/L$ experimental values as well as the curves calculated assuming ROM and Turner's model for the 50 vol. %-$Mn_{3.1}Zn_{0.5}Sn_{0.4}N$/Ti composite. The thermal expansion was reduced, even negative

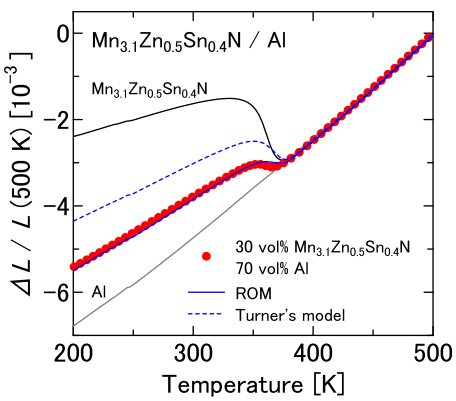

FIG. 8. Experimental plots of linear thermal expansion as well as curves calculated by assuming rule of mixture (ROM) and Turner's model for 30 vol. %-$Mn_{3.1}Zn_{0.5}Sn_{0.4}N$/Al composite.

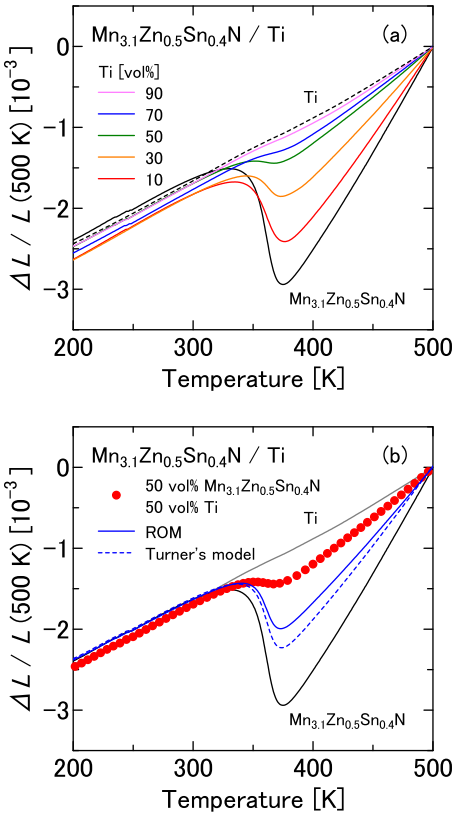

FIG. 9. (a) Linear thermal expansion of $Mn_{3.1}Zn_{0.5}Sn_{0.4}N$/Ti composite for various $Mn_{3.1}Zn_{0.5}Sn_{0.4}N$ filler loading. (b) Experimental plots of linear thermal expansion, and curves calculated by assuming the ROM and Turner's model for 50 vol. %-$Mn_{3.1}Zn_{0.5}Sn_{0.4}N$/Ti composite.

($\alpha = -2.2$ ppm K^{-1}), at $T = 340$–370 K ($\Delta T = 30$ K). The obtained α_c does not lie within the range predicted by the simple models, but is even larger than the upper bound, ROM.

One might regard the undesirable chemical reaction between the matrix and the thermal-expansion compensator as the origin of the unreasonably high thermal expansion of the composites. However, such a presumption is contradicted by the following results. The XRD profile after sintering is a superimposition of the individual patterns of the matrix and the compensator (Fig. 10), providing evidence against the chemical reaction during fabrication. Observations conducted using a microscope (Fig. 11) show a clear distinction between the matrix (matte gray) and the compensator (glossy gray), although the part of voids (black) increased compared with the Mn-Zn-Sn-N/Al composite. In contrast to the Al composite, the chemical reaction between the matrix and the compensator is not active for the Ti composite at 650 °C. The activation temperature of the chemical reaction between the matrix and the NTE manganese nitrides depends strongly on the matrix. The reason for the unreasonably poor performance of the thermal-expansion compensator will be addressed later.

D. Mn-Zn-Sn-N/Cu composite

For the third matrix, we used Cu. The NTE manganese nitrides/Cu composites were fabricated by Ding *et al.* using powder metallurgy, in which $Mn_3Cu_{0.5}Sn_{0.5}N$ and $Mn_3Cu_{0.5}Ni_{0.5}N$ were used as the NTE filler.[35] They achieved low

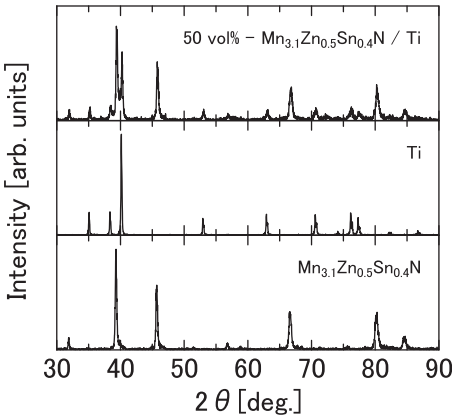

FIG. 10. X-ray diffraction profiles of 50 vol. %-$Mn_{3.1}Zn_{0.5}Sn_{0.4}N$/Ti composite as well as pure Ti and $Mn_{3.1}Zn_{0.5}Sn_{0.4}N$.

expansion of $\alpha = 0.47\,\text{ppm}\,\text{K}^{-1}$ at $T = 290$–$320\,\text{K}$ ($\Delta T = 30\,\text{K}$). Here, we fabricated the Cu matrix composites at $T_s = 550\,^\circ\text{C}$ with a fixed sintering time $t_s = 7$ min. The mixing ratio of $Mn_{3.1}Zn_{0.5}Sn_{0.4}N$ was 40 vol. %. Figure 12 displays $\Delta L(T)/L$ for the 40 vol. %-$Mn_{3.1}Zn_{0.5}Sn_{0.4}N$/Cu composite. The curves calculated assuming ROM and Turner's model are also shown. The thermal expansion was reduced, even negative ($\alpha = -7.8$ ppm K^{-1}), at $T = 340$–$370\,\text{K}$ ($\Delta T = 30\,\text{K}$). The obtained $\Delta L(T)/L$ of the Mn-Zn-Sn-N/Cu composite almost coincides with the ROM estimation.

The XRD profile after sintering is a superimposition of the individual patterns of the matrix and the compensator (Fig. 13), showing avoidance of excessive reaction between the matrix and the compensator. From the microscope observation (Fig. 14), we can draw a clear distinction between the matrix (metallic brown) and the compensator (glossy gray). We also recognize remarkably fewer voids (black) than in the Al [Fig. 5(a)] or Ti (Fig. 11) composites.

Although the chemical reaction between the matrix and the compensator is expected to proceed at 550 °C for the Al composite, it is not so active for the Cu composite at this temperature, similar to the Ti composite. Although the voids were reduced, the obtained $\Delta L(T)/L$ of the Mn-Zn-Sn-N/Cu composite almost coincides with the ROM estimation. Suppression of thermal expansion beyond the volume fraction was not confirmed for the Cu composite.

IV. DISCUSSION

A. Composite performance

The giant NTE over $\alpha = -30$ ppm K^{-1} of the manganese nitride expands our capability of thermal-expansion control and achieves widely various α, even negative values, in MMCs. Fine tuning of α in the negative region is possible because the negative α is realized using lower filler loading than that of other NTE materials. The filler loading quantities necessary for negative α were respectively, less than 30 vol. %, 50 vol. %, and 40 vol. % for these Al, Ti, and Cu composites. In many cases, it is difficult for other NTE materials to achieve negative α in a MMC.[5,6,16,17] For ZrW_2O_8/Al[12] and ZrW_2O_8/Cu[13] composites, α became almost zero or even slightly negative at last for the 75 vol. % filler loading. Another example of negative α is a case of the $Sc_2W_4O_{12}$-core/Cu-shell composite, in which the volume fraction of $Sc_2W_4O_{12}$ showing NTE is extremely high, roughly over 80 vol. %.[36] Finely tuned negative α is in the present composites enables us, for example, to athermalize a fiber Bragg grating.[37] Low filler loading also minimizes the unfavorable reduction of thermal conductivity of an MMC.

Another merit of this method is the high reproducibility of thermal expansion. We can reproducibly adjust the thermal expansion of the composite to a particular value by controlling the mixing ratio of the matrix and the compensator. That adjustment is possible because of the powder metallurgy in which the mixing ratio can be controlled finely. The high reproducibility enables us to make a functionally graded material in which thermal expansion changes gradually from a matrix-rich (high α) region to a compensator-rich (low α) region.

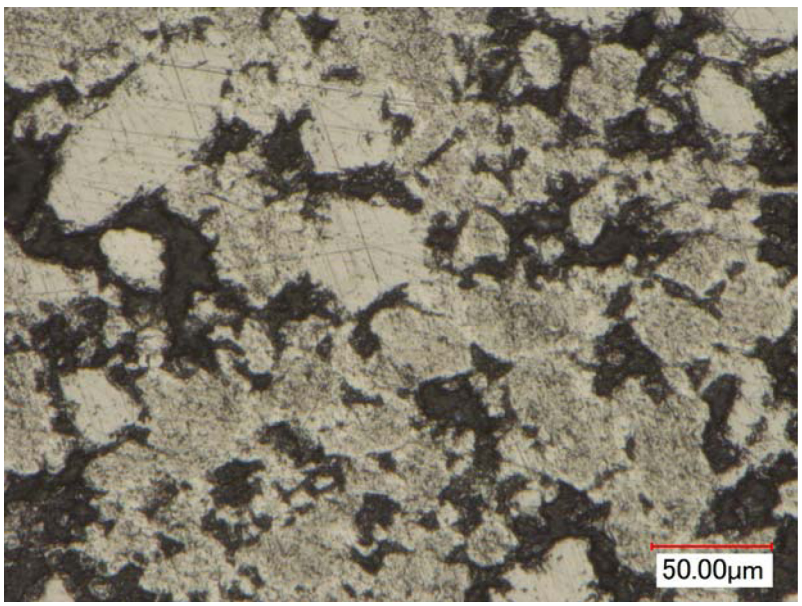

FIG. 11. Microscopic image of 50 vol. %-$Mn_{3.1}Zn_{0.5}Sn_{0.4}N$/Ti composite.

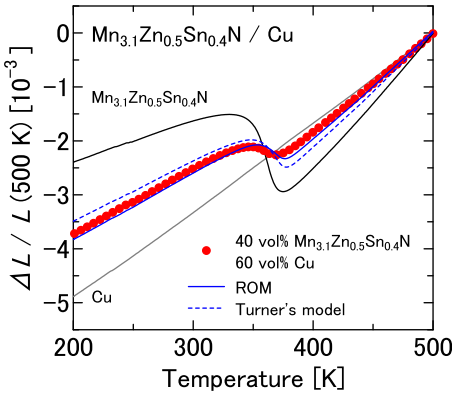

FIG. 12. Experimental plots of linear thermal expansion as well as curves calculated by assuming ROM and Turner's model for 40 vol. %-$Mn_{3.1}Zn_{0.5}Sn_{0.4}N$/Cu composite.

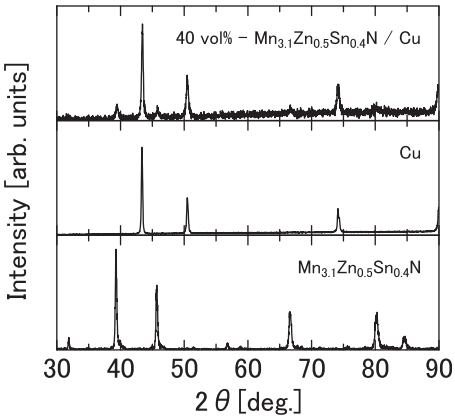

FIG. 13. X-ray diffraction profiles of 40 vol. %-$Mn_{3.1}Zn_{0.5}Sn_{0.4}N$/Cu composite as well as pure Cu and $Mn_{3.1}Zn_{0.5}Sn_{0.4}N$.

Thermal-expansion properties such as a working temperature can be altered more drastically by changing the thermal-expansion compensator, although unique composition $Mn_{3.1}Zn_{0.5}Sn_{0.4}N$ has been used as a representative in this study. For example, we achieved extremely low thermal expansion at just room temperatures in the 50 vol. %-$Mn_{3.27}Zn_{0.45}Sn_{0.28}N$/Al composite (Fig. 15). It shows NTE of $\alpha = -0.3$ ppm K^{-1} at $T = 275-310$ K ($\Delta T = 35$ K).

B. Sintering temperature

Sintering (fabrication) temperature T_s is the most important parameter for forming the NTE manganese nitride/metal matrix composites. Here, T_s is expected to be higher than the temperature at which the pure metal matrix can be sintered and is expected to be lower than the temperature at which the chemical reaction between the nitride and the matrix excessively proceeds. A lack of a chemical reaction is also unfavorable because the interfacial chemical bonding is necessary for solidification of the composite.

The temperature at which the interfacial chemical reaction proceeds excessively varies greatly, according to the kind of metal matrix. For the Al composite, the reaction becomes active at 520 °C. Therefore, T_s is expected to be lower than 520 °C. For the Ti and Cu composites, however, the interfacial chemical reaction is well controlled even at temperatures higher than 520 °C. Therefore, we used 650 °C and 550 °C as T_s, respectively.

It is important to ascertain whether the manganese nitride itself can be sintered at the T_s used for this study. In this study, the grains of the thermal-expansion compensator are sintered between themselves for the Ti and Cu composites but not for the Al composite. This difference is reflected in the difference in the realized filler loading range. We failed to fabricate the Al composites with higher filler loading than 70 vol. % because of their low solidification, although we realized almost all the filler loading range for the Ti composite [Fig. 9(a)]. This is expected to affect the mechanical properties of the composites, which has yet to be confirmed.

C. Lattice-parameter misfit

For the Al and Cu composites, the obtained $\Delta L(T)/L$ lies between the two theoretical bounds. It is close to the upper α_c bound. For the Ti composite, however, the obtained

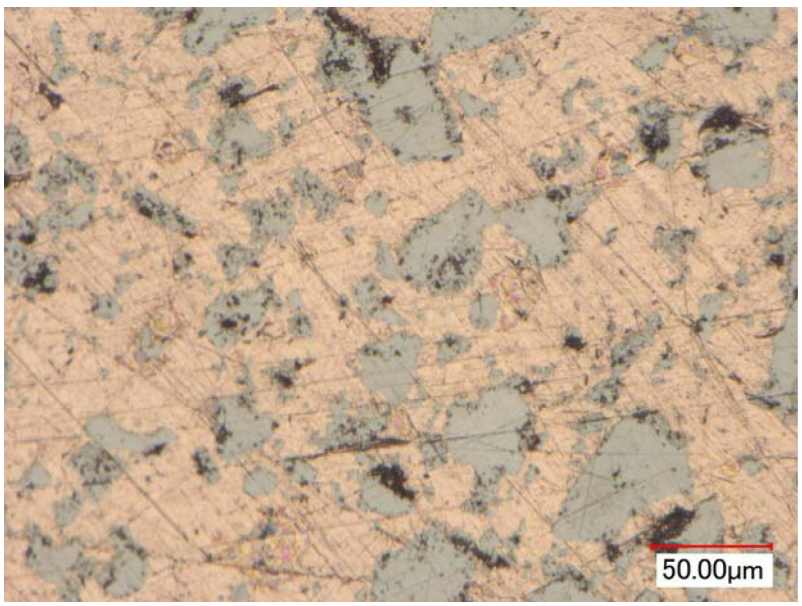

FIG. 14. Microscopic image of 40 vol. %-$Mn_{3.1}Zn_{0.5}Sn_{0.4}N$/Cu composite.

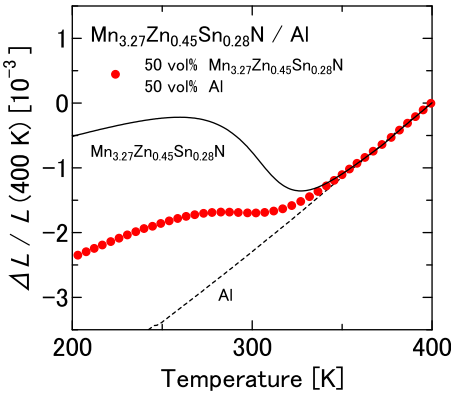

FIG. 15. Extremely low thermal expansion at room temperature of 50 vol. %-$Mn_{3.27}Zn_{0.45}Sn_{0.28}N$/Al composite.

$\Delta L(T)/L$ does not fall within the range of the two theoretical bounds, even larger than the upper α_c bound. The difference is discussed here in terms of lattice-parameter misfit between the matrix and the compensator.

The lattice parameters of the metal matrices and the thermal-expansion compensators before and after forming composites are presented in Table III. For all the composites, the lattice parameters are changed negligibly by forming a composite, showing that the chemical reaction between the matrix and the compensator is suppressed except in the narrow interfacial region, and their individual properties are retained. Aluminum and copper are cubic with respective lattice parameters of 4.053 Å and 3.616 Å, whereas titanium is hexagonal with lattice parameters of $a = 2.954$ Å and $c = 4.690$ Å. Because the manganese nitride compensator is cubic with a lattice parameter of 3.969 Å, the lattice-parameter misfit increases in the sequence Al, Cu, and Ti. The low thermal expansion compensation in the Ti composites can be explained by considering inhibition of stable interfacial bonding between the matrix and the compensator because of their lattice-parameter misfit.

D. Voids and composite performance

Voids still exist in these MMCs. Numbers of voids are roughly estimated from image analysis of the microscope observation, increasing in the sequence Cu (3 vol. %), Al (10 vol. %), and Ti (33 vol. %) composites. The estimation for the Cu composite shows quantitative agreement with the estimation using Archimedes principle. Because the Ti composite with large lattice-parameter misfit contains large amount of voids, the lattice-parameter misfit can be one of the origins of voids. Nevertheless, the lattice-parameter misfit cannot be a dominant factor of voids, because the Cu composite contains only a few vol. % of voids, though the lattice-parameter misfit is larger than the Al composite. Mechanical properties such as Young's modulus E and Vickers hardness H_V also seem to be irrelevant, because we recognize no systematic relationship between the amount of voids and the mechanical properties (Table I).

TABLE III. Lattice parameters of components before and after forming composites.

		Lattice parameter (Å)	
MMC	Component	Before	After
Al-composite	Al	4.053	4.046
	$Mn_{3.1}Zn_{0.5}Sn_{0.4}N$	3.969	3.964
Ti-composite	Ti (a axis)	2.954	2.947
	Ti (c axis)	4.690	4.684
	$Mn_{3.1}Zn_{0.5}Sn_{0.4}N$	3.969	3.961
Cu-composite	Cu	3.616	3.614
	$Mn_{3.1}Zn_{0.5}Sn_{0.4}N$	3.969	3.962

The amount of voids increases with increasing particle size r of the matrix (Table II). We expect reduction of voids by reducing r, partly supported by our preliminary experiments for the Ti composites. However, we verified that the pure metal matrix powders were sintered with almost full density, even for Ti of $r = 45$ μm. Furthermore, it is noteworthy that the voids exist mainly in the interfacial region between the matrix and the compensator. The amount of voids seems to depend on the affinity between the matrix and the compensator.

Correlation between the voids and effect of reduced performance of thermal-expansion compensation is not straightforward. In principle, the presence of voids in a composite does not affect the thermal expansion because the voids have zero stiffness and therefore thermally induce no inner stress.[28] When the mixing ratios of the matrix and the compensator are extremely different and the framework of the composite is formed by the majority constituent, the contribution of the minority constituent to the thermal expansion is expected to be greatly reduced by the existence of voids. However, even for the comparable mixing ratio, 50 vol. % filler loading, the thermal expansion of the Ti composites is even higher than the upper bound that is predicted theoretically. By contrast, voids might degrade the ability of thermal-expansion compensator via poor interfacial bonding. Actual composites containing voids might not follow the theoretical predictions exactly because perfect interfacial bonding is assumed for the theoretical models of thermal expansion in a composite.

V. CONCLUDING REMARKS

Spark plasma sintering enabled us to reduce the fabrication temperature of the NTE manganese nitride/metal matrix composites to much lower than the melting point of the pure matrix. Consequently, we can use even high-melting-point metals including Ti as the matrix, although the manganese nitride thermal-expansion compensator is highly reactive with a molten metal. A wide range and high reproducibility of CTE are remarkable functionalities of these composites, enabling widely diverse applications in many fields of industry such as optical, processing, and electronics engineering.

Although we substantiated the control of the thermal expansion, the microscopic structure must be improved further. Voids and possible imperfections of interfaces between the matrix and the compensator are expected to degrade the mechanical and thermal-expansion properties of the composite. A quite large thermal-expansion mismatch exists

between the metal matrix and the giant NTE filler. A technology enabling us to form rich and stable interfacial chemical bonding presents a challenging problem for composite science and technology. The chemistry and physics of the interface deserve future investigations, which will eventually improve composite performance.

ACKNOWLEDGMENTS

This work was supported in part by the Ministry of Education, Culture, Sports, Science and Technology of Japan (Grant No. 22360291) and by NEDO, Japan (Grant No. 08A19009d).

[1]I. A. Ibrahim, F. A. Mohamed, and E. J. Lavernia, J. Mater. Sci. **26**, 1137 (1991).
[2]S. Elomari, M. D. Skibo, A. Sundarrajan, and H. Richards, Compos. Sci. Technol. **58**, 369 (1998).
[3]C. P. Wong and R. S. Bollampally, J. Appl. Polym. Sci. **74**, 3396 (1999).
[4]A. W. Sleight, Inorg. Chem. **37**, 2854 (1998).
[5]W. D. Fei and L. D. Wang, Mater. Chem. Phys. **85**, 450 (2004).
[6]Z. W. Xue, L. D. Wang, Z. Liu, and W. D. Fei, Scr. Mater. **62**, 867 (2010).
[7]A. Borrell, O. García-Moreno, R. Torrecillas, V. García-Rocha, and A. Fernández, Sci. Technol. Adv. Mater. **13**, 015007 (2012).
[8]C. N. Chu, N. Saka, and N. P. Suh, Mater. Sci. Eng. **95**, 303 (1987).
[9]T. A. Mary, J. S. O. Evans, T. Vogt, and A. W. Sleight, Science **272**, 90 (1996).
[10]H. Holzer and D. C. Dunand, J. Mater. Res. **14**, 780 (1999).
[11]S. Yilmaz, Compos. Sci. Technol. **62**, 1835 (2002).
[12]A. Matsumoto, K. Kobayashi, T. Nishio, and K. Ozaki, Mater. Sci. Forum **426–432**, 2279 (2003).
[13]D. K. Balch and D. C. Dunand, Metall. Mater. Trans. A **35**, 1159 (2004).
[14]L. M. Sullivan and C. M. Lukehart, Chem. Mater. **17**, 2136 (2005).
[15]J. Tani, H. Kimura, K. Hirota, and H. Kido, J. Appl. Polym. Sci. **106**, 3343 (2007).
[16]X. Yan, X. Cheng, G. Xu, C. Wang, S. Sun, and R. Riedel, Materialwiss. Werkstofftech. **39**, 649 (2008).
[17]J. E. Trujillo, J. W. Kim, E. H. Lan, S. Sharratt, Y. S. Ju, and B. Dunn, J. Electron. Mater. **41**, 1020 (2012).
[18]K. Takenaka and H. Takagi, Appl. Phys. Lett. **87**, 261902 (2005).
[19]A. E. Phillips, A. L. Goodwin, G. J. Halder, P. D. Southon, and C. J. Kepert, Angew. Chem., Int. Ed. **47**, 1396 (2008).
[20]Y. Wu, A. Kobayashi, G. J. Halder, V. K. Peterson, K. W. Chapman, N. Lock, P. D. Southon, and C. J. Kepert, Angew. Chem., Int. Ed. **47**, 8929 (2008).
[21]B. K. Greve, K. L. Martin, P. L. Lee, P. J. Chupas, K. W. Chapman, and A. P. Wilkinson, J. Am. Chem. Soc. **132**, 15496 (2010).
[22]M. Azuma, W. T. Chen, H. Seki, M. Czapski, S. Olga, K. Oka, M. Mizumaki, T. Watanuki, N. Ishimatsu, N. Kawamura, S. Ishiwata, M. G. Tucker, Y. Shimakawa, and J. P. Attfield, Nat. Commun. **2**, 347 (2011).
[23]M. B. Jakubinek, C. A. Whitman, and M. A. White, J. Therm. Anal. Calorim. **99**, 165 (2010).
[24]K. Takenaka, Sci. Technol. Adv. Mater. **13**, 013001 (2012).
[25]K. Takenaka, K. Asano, M. Misawa, and H. Takagi, Appl. Phys. Lett. **92**, 011927 (2008).
[26]H. Imai, M. Okaji, T. Kishii, H. Sagara, H. Aikawa, and R. Kato, Int. J. Thermophys. **11**, 937 (1990).
[27]K. Takenaka and H. Takagi, Appl. Phys. Lett. **94**, 131904 (2009).
[28]T. W. Clyne and P. J. Withers, *An Introduction to Metal Matrix Composites* (Cambridge University Press, 1993).
[29]P. S. Turner, J. Res. Natl. Bur. Stand. **37**, 239 (1946).
[30]Y. Nakamura, K. Takenaka, A. Kishimoto, and H. Takagi, J. Am. Ceram. Soc. **92**, 2999 (2009).
[31]Y. Sun, C. Wang, Y. C. Wen, K. G. Zhu, and J. T. Zhao, Appl. Phys. Lett. **91**, 231913 (2007).
[32]R. J. Huang, L. F. Li, F. S. Cai, X. D. Xu, and L. H. Qian, Appl. Phys. Lett. **93**, 081902 (2008).
[33]Z. H. Sun, X. Y. Song, F. X. Yin, L. X. Sun, X. K. Yuan, and X. M. Liu, J. Phys. D: Appl Phys. **42**, 122004 (2009).
[34]T. Hamada and K. Takenaka, J. Appl. Phys. **109**, 07E309 (2011).
[35]L. Ding, C. Wang, Y. Y. Na, L. H. Chu, and J. Yan, Scr. Mater. **65**, 687 (2011).
[36]Q. Q. Liu, J. Yang, X. N. Cheng, G. S. Liang, and X. J. Sun, Ceram. Int. **38**, 541 (2012).
[37]A. Sakamoto, T. Matano, and H. Takeuchi, IEICE Trans. Electron. **E83C**, 1441 (2000).